International Journal of Emerging Engineering Research and Technology
Volume 2, Issue 4, July 2014, PP 123-133
ISSN 2349-4395 (Print) & ISSN 2349-4409 (Online)

A Medical Volume Segmentation Technique Using 3D Discrete Wavelet Transform (DWT)

M.Nivas
Research Scholar,
Computer Science and Engineering
Bharath University,
Chennai, T.N., India.

Dr.M.Ramakrishnan
Research Supervisor,Prof. & Head,
Department of Information Technology,
Velammal Engineering College,
Chennai, T.N., India.

Abstract: *3D volume segmentation aims at separating the voxels into 3D objects (sub-volumes) which signify significant physical entities. MRA permits for the conservation of an image according to definite levels of resolution or blurring. The excellence of this technique makes it valuable in image compression, de-noising, and classification or segmentation. This paper concentrates on the implementation of a medical volume segmentation technique using 3D MRA techniques. Therefore, 3D discrete curvelet transform is proposed and compared with the discrete wavelet transform (DWT). An evaluation study has been performed to estimate 2D and 3D techniques which disclose that 3D approaches can precisely discover the region of interest in both phantom and real data.*

Keywords: *Segmentation, Medical images, Multi- Resolution analysis, 3D image processing, Discrete wavelet transform, Discrete curvelet transform.*

1. INTRODUCTION

Volume segmentation allots the voxels in 3D images into partitions or 3D regions that characterize significant physical units. The objective is to differentiate among diverse regions in the 3D volume and wrap the extracted contours from the whole volume. The categorization of Voxels into regions is done according to definite region to which the voxels fit in, and some shared, predefined possessions. Those voxels encompass a secluded or segmented Object of Interest (OOI) from the input volume. Segmentation can be physically carried out by a human expert who merely inspects an image, decides on borders between regions, and classifies each region. This is perchance the most trustworthy and precise scheme of image segmentation since the human visual system is massively complex and well adapted to the mission [1]. However when the image in issue is volumetric, performing this task does become really complex. There are numerous further existing techniques developed for medical image segmentation, including Multiresolution Analysis (MRA), statistical methods, thresholding and clustering based techniques. In clustering method each pixel in an image is classified into the suitable cluster, and then these clusters are mapped to exhibit the segmented images. For grouping each pixel into a definite number of clusters depending on the image histogram, a certain clustering standard can be implemented [1] [2].

Medical images can as well be segmented by means of thresholding techniques by partitioning their intensities. When images contain dissimilar structures with distinguishing intensities, thresholding affords an easy way for attaining segmentation. In general, the thresholds are developed based on visual evaluation of the resulting segmentation [3]. MRA permits for the conservation of an image according to definite levels of resolution or blurring. Multiresolution quality has made the wavelets being useful in image compression, de-noising, and classification. The objective of this paper is to precisely distinguish the region of interest (ROI) in the experimental data by means of different 2D and 3D schemes.

In [18], 3D DWT has been proposed for segmentation of medical volumes and they stated that the 3D Curvelet transform has not been implemented for the medical image segmentation. This could extract the curves which are occurring along many slices in medical volumes and it can offer more accurate results so far achieved in the medical segmentation. Therefore, this paper proposes the 3D discrete Curvelet transform for the segmentation of medical volumes and compares the performance with the 3D DWT method. A brief literature survey of similar existing schemes is presented in section 2. The mathematical background of 3D image processing is explained in section 3. In section 4, volume segmentation using 3D discrete wavelet transform (3D-DWT) is detailed. Section 5 deals with the proposed 3D Discrete curvelet transform. A comparison study has been executed to estimate 2D and 3D techniques presented in section 6 where the 3D DWT is applied on real medical data and proposed phantom data. Section 6 presents the conclusion of the work.

2. LITERATURE SURVEY

Segmentation is a major phase in the segmentation process of medical images, where user intervention is recommended as an additional source of information. This method leverages the proficient knowledge of users to produce accurate segmentation of anatomical structures, which aids measurement and diagnosis of various diseases. Numerous methods have been proposed for the segmentation however it can be further classified into the following categories [4]. They are edge based segmentation, region based segmentation, statistical approaches, graph cut based approaches and deformable modes based approaches.

Won Hwa Kim et.al have presented a method [5] to provide the multi-resolutional capabilities through non-Euclidean wavelet theory for a range of 3-D shape analysis problems in Computer Vision. They have shown that the descriptors derived from the dual domain representation provided native multi-resolution behavior to characterize the local or global topology in the region of vertices. They have proposed algorithms for perceptually meaningful shape mesh segmentation, interest point detection and surface alignment independently. Moreover, they have presented a set of comparison results on a large shape segmentation benchmark and derived a uniqueness theorem for the surface alignment problem.

Divya Kaushik et.al presented a succinct article [6] of various segmentation methodologies applied for medical image processing. It was noticeable that the utilization of the clustering methods in medical images is the recognition of damaged areas in tissues. The well-known Genetic Algorithm was applied for the segmentation of tissues in the medical MRI images.

Xinjian Chen et.al have proposed a 3-D automatic anatomy segmentation method [7] to develop their complementary strengths by combining the active appearance model (AAM), live wire (LW), and graph cuts (GC) ideas. They have constructed the AAM and trained the LW cost function and GC parameters. Moreover, a novel algorithm was proposed in the recognition phase to enhance the conventional AAM matching method. This method was combined the AAM and LW methods effectively, which has resulted in the oriented AAM (OAAM). Moreover, a multiobject strategy was utilized to help in the object initialization phase. The proposed method has consumed 5 minutes to segment one organ from the medical image.

3. MATHEMATICAL BACKGROUND

The main general way for developing 3D data set in medical applications is from tomographic devices such as computed tomography scanners (CT). Such devices are proficient in slicing an object in a physical sectioning. 3D data of those devices can be regarded as parallel slices loaded to generate a 3D volume. Each one of those slices is a 2D medical image which characterizes a particular section from the human body. By means of an algorithm given in [8], all the slices are stacked to produce a 3D matrix which estimates the 3D medical volume. The mathematical backgrounds of the proposed medical volume segmentation scheme are given in the following sub sections.

3.1. Thresholding

Scalar images can be segmented by means of thresholding techniques by partitioning image intensities. This method tries to decide an intensity value that can partition the signal into a preferred number of classes. As explained in pseudocode 1, the segmentation can be attained by clustering all pixels with intensities higher than the threshold value into one class, and the remaining pixels into another class. In numerous applications, the threshold values are selected based on the volume histogram basis and Multi-thresholding takes place when more than one threshold value is established [9][10].

3.1.1. Pseudo code for 2D-Thresholding

```
if pixel value is less than or equal to the threshold value then
set pixel value is equal to zero
end if
```

3D thresholding technique differs from the 2D methodology in the nature of thresholding process since 3D applies thresholding on all pixels in the volume rather than that in the plane. The pseudo code for 3D thresholding is provided in the section 3.1.1.

3.1.2. Pseudo Code for 3D-Thresholding

```
Stack 3D data set into V
[x y z]= size (V)
%apply thresholding process for each pixel in the volume
for i = 1 to x do
for j = 1 to y do
for k = 1 to z do
if Pixel value is less than or equal to the Threshold value then
set Pixel value is equal to zero
end if
end for
end for
end for
```

3.2. Wavelet Transform

DWT performs a convolution operation of target function with wavelet kernels to gain wavelet coefficients denoting the offerings of wavelets in the function at diverse scales and orientations. DWT can be implemented as a set of filter banks, consisting of a high-pass and low-pass filters. In standard wavelet decomposition, the output from the low pass filter can then further be decomposed; this process of decomposition is performed recursively as depicted in figure. 1, DWT can be mathematically expressed by equations (1) and (2) [11]:

$$x^i(n) = \sum_{m=0}^{M-1} l_p(m).x^{i-1}(2n-1), 0 \le n < N_i, \quad (1)$$

$$y^i(n) = \sum_{m=0}^{M-1} h_p(m).y^{i-1}(2n-1), 0 \le n < N_i. \quad (2)$$

The coefficients $x^i(n)$ and $y^i(n)$ refer to approximation and detailed components in the signal at decomposition level i respectively. The $l_p(m)$ and $h_p(m)$ signify the coefficients of low-pass and high-pass filters correspondingly. Wavelet transform decomposes the signal into a set of resolution associated visions. The wavelet decomposition of an image forms at each scale i, a set of coefficient values w_i, with an overall mean of zero. This set of coefficient values w_i includes the equivalent number of voxels as the novel 3D volume, and hence, this wavelet transform is superfluous [12][13]. A non-decimated or surplus wavelet transform is helpful for the discovery of excellent features within the signal.

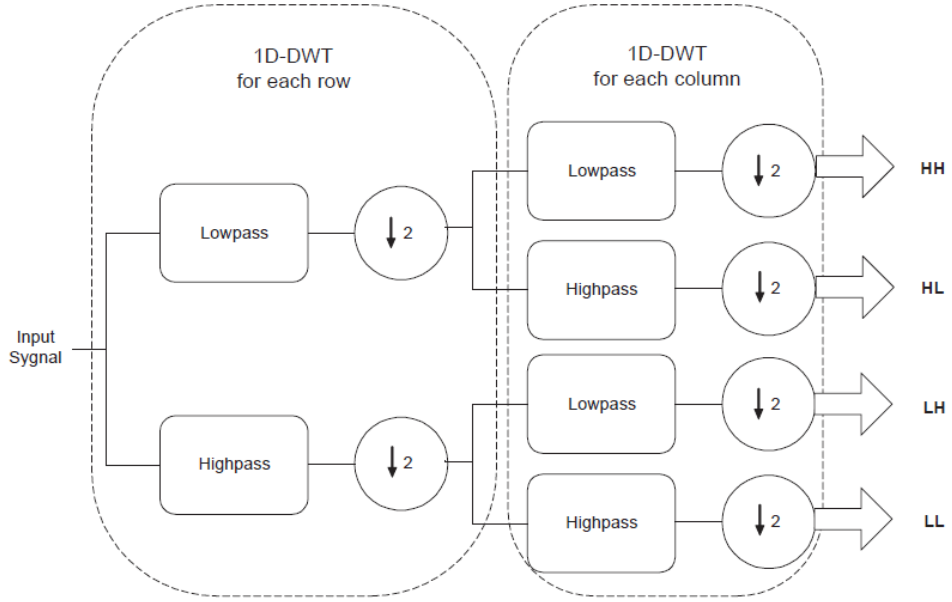

Figure 1. *2D Haar filter architecture*

For the instant of images, the one-dimensional DWT can be willingly widened to 2D in two modes. In standard two dimensional wavelet decomposition the image is fully decomposed in row wise, while the output being entirely decomposed column wise. However in the non-standard wavelet decomposition, the entire rows are decomposed by one decomposition level followed by one decomposition level of the columns [14] [15]. The pseudocode of which is given in section 3.2.1. Fig. 2 depicts the procedure of employing 2D-DWT of Standard and non-standard wavelet transform.

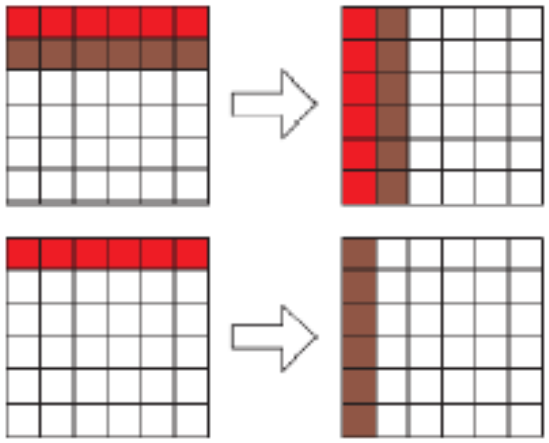

Figure 2. *Standard and non-standard wavelet transform.*

3.2.1. Pseudocode for Standard and Non-standard decomposition

Standard Decomposition

```
for each row
    {do the one-dimensional decomposition}
end
for each column
    {do the one-dimensional decomposition}
end
```

Non-Standard Decomposition

```
for each row %% or each column
```

{do the one-dimensional decomposition for one row}

{do the one-dimensional decomposition for each column}

end

4. 3D DISCRETE WAVELET TRANSFORM

It has been explained in section 3.2 that 2D-DWT is a simplification of 1D-DWT on all rows and columns using standard or non-standard decomposition. Applying 3D-DWT is not simple, the distinction between 2D images and 3D volumes is considered as the third dimension (depth or Z-axis). The 3D-DWT obtained after applying the 3D transform is depicted in figure 3, where the initial volume is transformed into 8 octants (features) in the wavelet domain which are:

LLL - LLH - LHL- LHH - HLL - HLH - HHL - HHH.

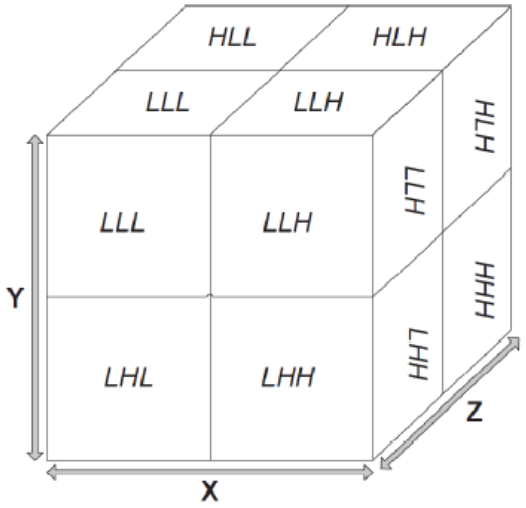

Figure 3. *3D volume in wavelet domain*

Mathematically, 3D-DWT is the method of applying 1D DWT on each vector in Z-axis which has an equivalent X-axis and Y-axis coordinates after applying 2D-DWT for all embracing frames, where each frame pixels have the similar Z-axis values. The pseudocode for applying 3D-DWT on 3D data set is given in section 4.1.

4.1. Pseudocode for 3D DWT on 3D Data Set

Stack 3D data set into V // V is data volume

[x y z] = size (V) // returns the size of 3D data

for k = 1 to z do

apply 2D-DWT for each plane in Z-axis

end for

for i = 1 to x do

for j = 1 to y do

apply 1D-DWT for each vector in XY plane

end for

end for

5. 3D DISCRETE CURVELET TRANSFORM

The 3D curvelet transform is anticipated to maintain the properties of the 2D transform. Most significantly, the frequency support of a 3D curvelet shall be confined near a wedge which pursues the parabolic scaling property. One can confirm that this involves that the 3D curvelet frame is a sparse

basis for denoting functions with surface like singularities (which is of co dimension one in 3D) however or else smooth. For the continuous transform, the frequency content is windowed as follows. The radial window evenly extracts the frequency near the dyadic corona $\{2^{j-1} \leq r \leq 2^{j+1}\}$, this is equivalent as the radial windowing employed in 2D. For each scale j, the unit sphere S^2 which signifies all the directions in R^3 is divided into O ($2^{j/2}.2^{j/2}$) = O (2^j) and the squares of which make a partition of unity on S^2 (see Figure 4).

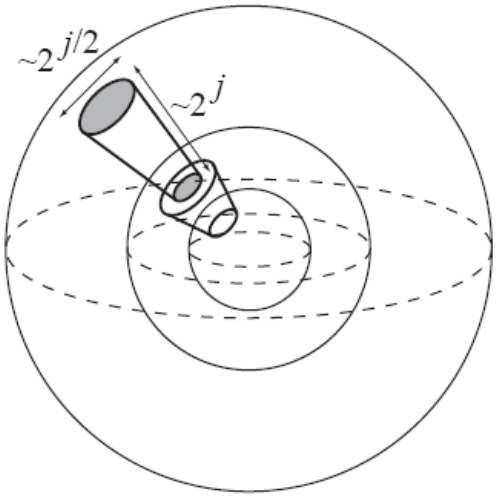

Figure 4. *Schematic plot for the frequency tilting of continuous 3D curvelets.*

Like the 2D discrete transform, the 3D discrete curvelet transform acquires as input a 3D Cartesian grid of the form

f(n_1, n_2, n_3), 0≤ $n_1, n_2, n_3 < n$, and outputs a collection of coefficients $C^D\ (j, l, k)$ is defined by:

$$C^D\ (j, l, k) := \sum_{n_1,n_2,n_3} \mathrm{f}(n_1, n_2, n_3)\ \overline{\varphi^D_{j,l,k\ (n_1,n_2,n_3)}} \tag{3}$$

Where j, l ∈ Z and k= (k_1, k_2, k_3) (n_1, n_2, n_3)

Cartesian coronae of the form is employed here which is given in equation (4):

$$\widetilde{W}_{j0}(\omega) = \Phi_{j0}(\omega)\ and\ \widetilde{W}_j(\omega) = \sqrt{\Phi^2_{j+1}\ (\omega) - \Phi^2_j\ (\omega)}\ \text{, j} \geq j0, \tag{4}$$

With $\Phi_j(\omega_1,\omega_2,\omega_3) = \Phi(2^{-j}\ \omega_1)\ .\ \Phi(2^{-j}\ \omega_2)\ .\ \Phi(2^{-j}\ \omega_3)$. where the function Φ is the same as previously said.

Coarsest Scale: j = $j0$. The frequency window $\widetilde{U}_{j_0,0}$ is again defined by

$$\widetilde{U}_{j_0,0}(\omega) = \widetilde{W}_{j0}(\omega)$$

Suppose $U_{j_0,0}$ is carried in a rectangular box of integer size $L_{1,j_o} \times L_{2,j_o} \times L_{3,j_o}$. Fourier transforms represent the discrete curvelets at the coarsest level as specified below

$$\hat{\varphi}^{\boldsymbol{D}}_{j_0,0,k}(\omega) = \widetilde{U}_{j_0,0}(\omega)\ .\exp\left[-2\pi i\left(k_1\omega_1/L_{1,j_o} + k_2\omega_2/L_{2,j_o} + k_3\omega_3/L_{3,j_o}\right)\right]/\sqrt{L_{1,j_o}\ .\ L_{2,j_o}\ .\ L_{3,j_o}} \tag{5}$$

for $0 \leq k_1 < L_{1,j_o}$, $0 \leq k_2 < L_{2,j_o}$ and $0 \leq k_3 < L_{3,j_o}$.

Fine Scale: $j_0 < j < j_e$.

Now there are six components in each Cartesian corona, one for every face of the unit cube. With an equivalent volume each component is frequently divided into $2^{j/2}.2^{j/2}$ wedges. Take for an instant

the first component (corresponding to $\omega_1 > 0$). Assume, for the *'l'*th wedge, $(1, \alpha_l, \beta_l)$ is the direction of the middle line of the wedge and its smooth angular window is defined as

$$\widetilde{V}_{j,l}(\omega) = \widetilde{V}\left(2^{j}/_{2} \,.\, \frac{\omega_2 - \alpha_l .\, \omega_1}{\omega_1}\right) . \widetilde{V}\left(2^{j}/_{2} \,.\, \frac{\omega_3 - \beta_l .\, \omega_1}{\omega_1}\right) \quad (6)$$

Where $\widetilde{V}$ is explained as before. For the remaining five components, the definition is alike by exchanging the roles of $\omega_1$with ω_2 or ω_3.

Final scale: j = j_e = log $_2$ (n/2). This final scale retrieves the highest frequency content of the 3D frequency cube. Alike, the 2D discrete transform, the final scale also has the wavelet-like basic function. The frequency window is

$\widetilde{U}_{j_e,0}(\omega) = \widetilde{W}_{je}(\omega)$.

The curvelets at this level are denoted by

$$\hat{\varphi}^{\boldsymbol{D}}_{j_e,0,k}(\omega) = \widetilde{U}_{j_e,0}(\omega) \,.\exp\left[-2\pi i\left(k_1\omega_1/L_{1,_{je}} + k_2\omega_2/L_{2,_{je}} + k_3\omega_3/L_{3,_{je}}\right)\right]/\sqrt{L_{1,_{je}} \,.\, L_{2,_{je}} \,.\, L_{3,_{je}}} \quad (7)$$

with $L_{1,_{je}} = L_{2,_{je}} = L_{3,_{je}} = n$ and $0 \leq k_1, k_2, k_3 < n$

5.1. Algorithm for 3D Discrete Curvelet Transforms

Step 1: Apply the 3D FFT and attain Fourier samples $\hat{f}(\omega_1, \omega_2, \omega_3)$, - $n/2 \leq \omega_1, \omega_2, \omega_3 < n/2$

Step 2: For each scale 'j' and angle 'l', form the product $\widetilde{U}_{j,l}(\omega_1, \omega_2, \omega_3)\hat{f}(\omega_1, \omega_2, \omega_3)$

Step 3: Wrap this product around the origin and obtain $\zeta\,(\widetilde{U}_{j,l}\hat{f})\;(\omega_1, \omega_2, \omega_3)$ where the range for $\omega_1, \omega_2\ and\ \omega_3$ is now

$-\frac{L_{1,j,l}}{2} \leq \omega_1 < \frac{L_{1,j,l}}{2}, -\frac{L_{2,j,l}}{2} \leq \omega_2 < \frac{L_{2,j,l}}{2}\ and\ -L_{3,_{j,l}}/2 \leq \omega_3 < L_{3,_{j,l}}/2,$ No wrapping is necessary at scales $j0$ and je

Step 4: Apply a $L_{1,_{j,l}}$ x $L_{2,_{j,l}}$ x $L_{3,_{j,l}}$ 3D inverse FFT to each $\zeta\,(\widetilde{U}_{j,l}\hat{f})$, hence collecting the discrete coefficients $C^D\,(j, l, k)$.

6. Results and Analysis

The proposed scheme has been tested using NEMA IEC body phantom data and real CT chest images. NEMA phantom consists of an elliptical water filled cavity with six spherical inserts suspended by plastic rods of inner diameters: 10, 13, 17, 22, 28 and 37 mm [16], this phantom is depicted in figure. 5 (a). Figure 5 (b) depicts one of the CT output slices which are stacked jointly to form the 3D volume as depicted in figure 4 (c).

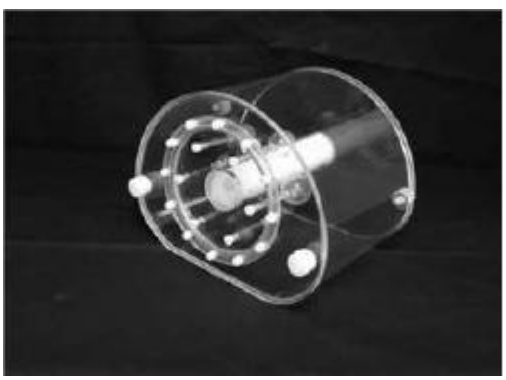

(a)

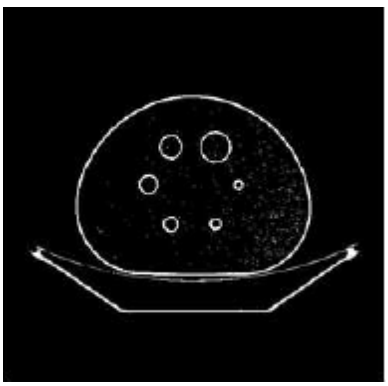

(b)

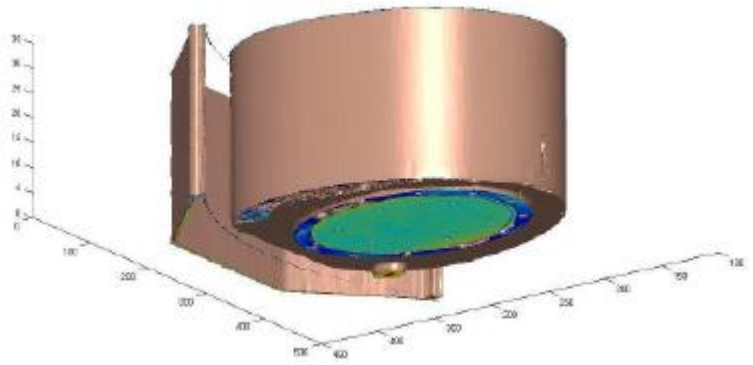

(c)

Figure 5. *(a) NEMA IEC body phantom [16], (b) 2D slice from a CT scanner, (c) 3D data set after stacking all slices using algorithm presented in [8].*

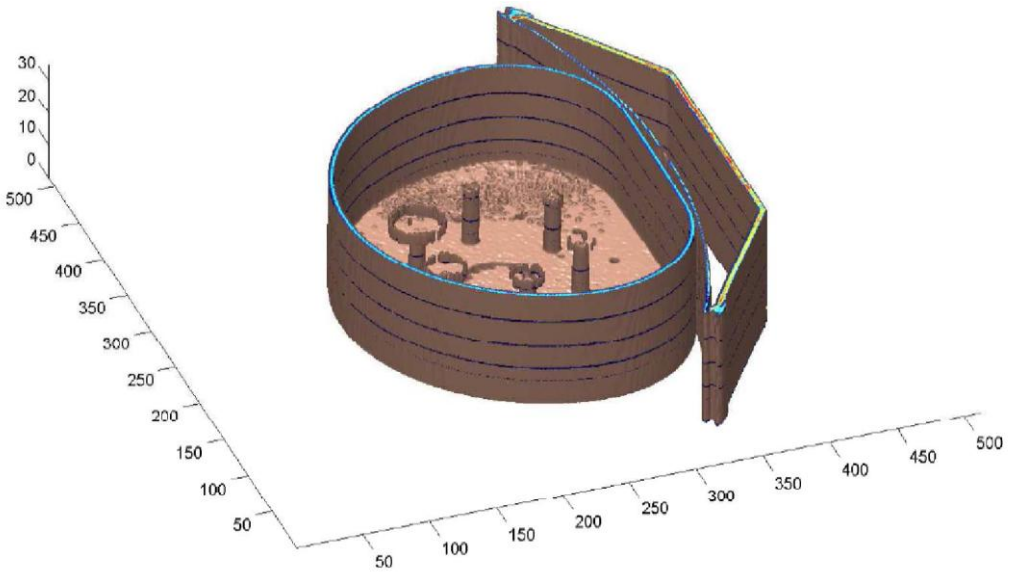

Figure 6. *Segmented volume using 3D-thresholding*

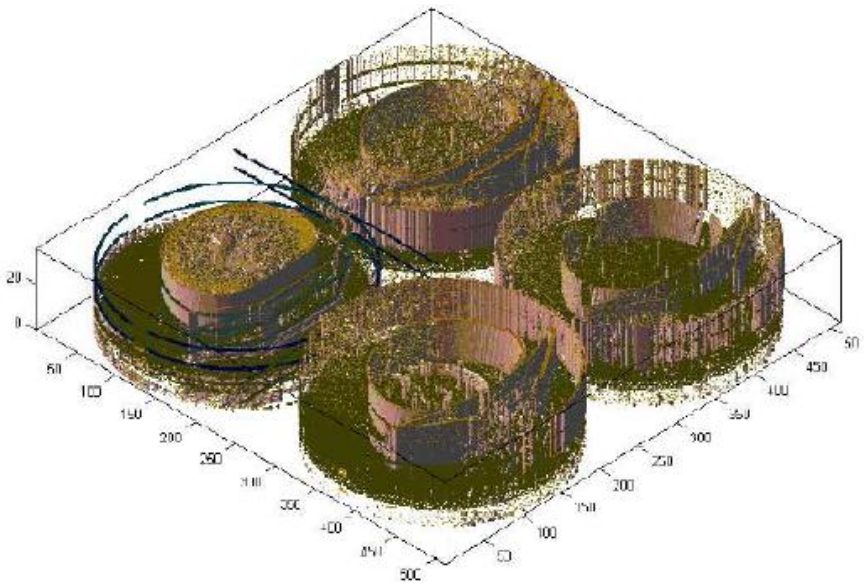

Figure 7. *3D-DWT for NEMA IEC body phantom*

Applying segmentation methods on 2D slices needs extra time compared to the time required for 3D volume. However the time involved in looking for the best slice that involves the spheres in full diameters is not necessary in 3D volume segmentation schemes. Volume segmentation for NEMA IEC using 3D thresholding is depicted in figure 6 and 3D-wavelet method is applied on the similar phantom data and the integrated spheres are detected as illustrated in figure 7.

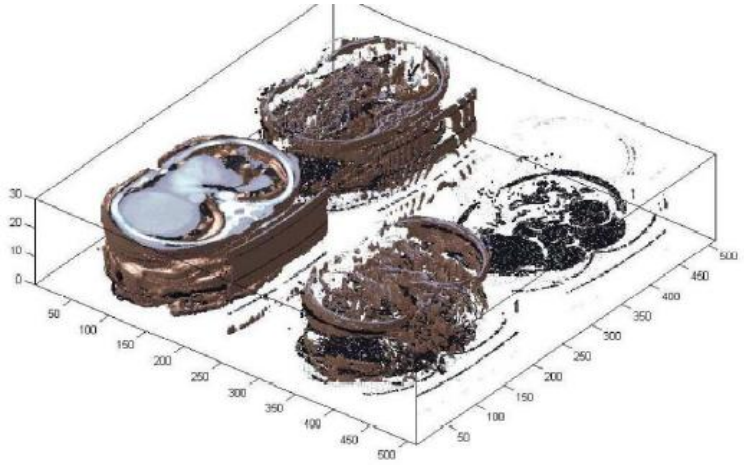

Figure 8. *3D-DWT for real CT images for the human chest.*

Another example of applying 3D-DWT on real CT images for the human chest [17] is demonstrated in figure 8, where the edges are discovered and the encompassing barriers can be observed from dissimilar angles.

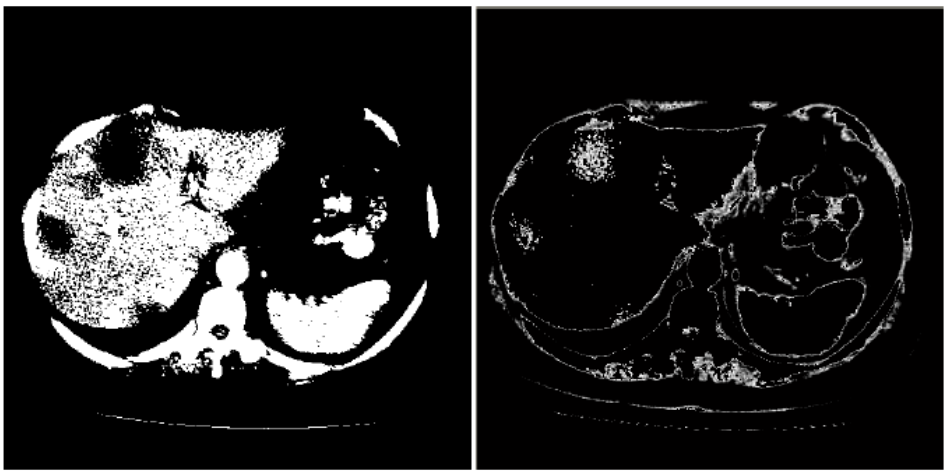

Figure.9 (a). Thresholding at t =77 **(b).** Inverse thresholding at t = 50

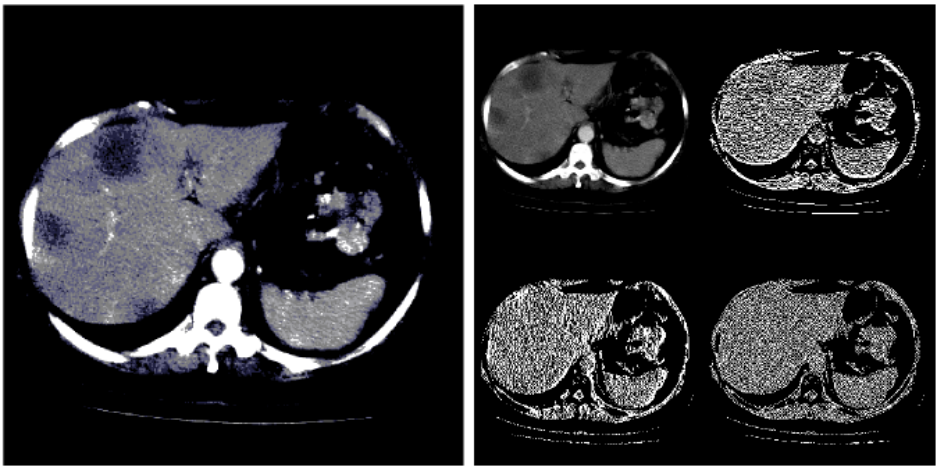

Figure.10 (a). *Clustering (6 classes)* **(b).** *Wavelet Transform*

Figure.9 shows that the segmented liver cancer using the implemented segmentation techniques. The ROI has been detected using most of the segmentation techniques with different quality. Both thresholding-based techniques shown in the figure.9 have detected the predefined liver cancer, but the problem with those methods is the data contouring loss, whereby a lot of image information has been missed in the transformed domain. As a result, thresholding-based techniques are of limited use in medical image segmentation, and are best used as pre-processing or post-processing steps beside other techniques. Clustering technique (used in Figure. 10 (a)) provided more accurate results compared to the thresholding techniques. The problem with using clustering in medical image segmentation lies in manual thresholding; multi-thresholding values have been set manually based on the human vision.

Table 1. *The error percentage of spheres diameters using different segmentation techniques*

Spheres (mm)	10	13	17	22	28
2D Thresholding	-4.8	-8.15	0.06	-0.36	1.07
2D DWT	-2.9	-2.46	1.35	0.82	0.29
3D Thresholding	0.59	0.77	0.17	1.11	2.20
3D DWT	-2.67	-1.93	-0.74	4.75	3.37
3D Discrete Curvelet Transform	-2.08	-1.56	-0.95	4.65	3.35

From table1, outer diameters have been used in the 3D medical volumes segmentation and the inner diameters error have been measured based on the thickness of the spheres edges. The error is increasing with respect to the increment of the sphere's diameter. However, the 3D techniques, DWT and DCT transforms have offered the similar error percentage. Moreover, the time and computation complexity of the 3D DCT transform is increased with the increasing of the spear's diameter.

7. CONCLUSION

An original and complicated segmentation system has been designed specifically for 3D data segmentation. This system was tested on phantom data obtained from BIN laboratory. The system was employed to enumerate tumors within the data of identified volume, and these results were compared with those achieved from 2D schemes. The 3D DCT method was proposed for the segmentation. This methodology offers proficient tumor quantification, helpful for staging and radiotherapy treatment development. The proposed system has been also experimented on other data set for the actual human chest images from a CT scanner [17]. But, the proposed 3D DCT method has been compared with the 3D DWT method in terms of error percentage. From the simulation results, we concluded that the 3D DCT method is better than the 3D DWT while diameter of the sphere is small. Nevertheless, the 3D DCT offers low performances than the 3D DWT in the higher diameters, which also increases the time and computational complexity. Therefore, 3D DWT can be efficiently used in all the sphere measures for the lower error percentage and complexity.

REFERENCES

[1] D. Montgomery, A. Amira and H. Zaidi, "Fully automated segmentation of oncological PET volumes using a combined multiscale and statistical model," Medical Physics, Vol. 34, Issue 2, pp. 722-736, 2007.

[2] P. Schelkens, A. Munteanu, J. Barbarien, M. Galca, X. Giro-Nieto, and J. Cornelis, "Wavelet Coding of Volumetric Medical Data sets," IEEE Transactions on Medical Imaging, 22(3), pp. 441–458, March 2003.

[3] D. Montgomery,"Multiscale Compression and Segmentation of Volumetric Oncological PET Imagery", Ph. D. thesis, Queens University - Belfast, 2006.

[4] Feng Zhao and Xianghua Xie, "An Overview of Interactive Medical Image Segmentation", Annals of the BMVA, Vol. 2013, pp.1–22, 2013

[5] Won Hwa Kim, Moo K. Chung and Vikas Singh, "Multi-resolution Shape Analysis via Non-EuclideanWavelets: Applications to Mesh Segmentation and Surface Alignment Problems", http://pages.cs.wisc.edu/wonhwa/.

[6] Divya Kaushik, Utkarsha Singh and Paridhi Singhal, "Medical Image Segmentation using Genetic Algorithm", International Journal of Computer Applications, Vol. 81, pp.10–15, 2013

[7] Xinjian Chen, Jayaram K. Udupa, Ulas Bagci, Ying Zhuge, and Jianhua Yao, "Medical Image Segmentation by Combining Graph Cuts and Oriented Active Appearance Models", IEEE Transactions on Image Processing, Vol. 21, pp.2035–2046, 2012

[8] Balter, "Dicom to 3 dimentional", Copyright (c) Pacific Northwest National Laboratory, 2009.

[9] P. Sahoo, S. Soltani and A.Wong, "A survey of thresholding techniques", Comput. Vision Graph. Image Process, 41 (1988), pp. 233-260.

[10] Amira, S. Chandrasekaran, D. Montgomery and I. Uzun," A segmentation concept for positron emission tomography imaging using multiresolution analysis," Neurocomputing, Elsevier, 2008.

[11] Uzun and A. Amira, "Design and FPGA Implementation of Finite Ridgelet Transform," International symposium on circuits and systems, 5826-5829, vol. 6, 2005.

[12] E. Stollnitz, T. DeRose and D. Salesin, "Wavelets for Computer Graphics," A Primer, Part 1, 2002.

[13] Haar, "Zur Theorie der Orthogonalen Funkt Ionensysteme", Mathematische Annalen, 1910, pp. 331- 371.

[14] R. Gonzalez and R.Woods, "Digital Image Processing", second ed., Prentice-Hall, Englewood Cliffs, NJ, 2001.

[15] Jensen and A. la Cour-Harbo, "Ripples in Mathematics: The Discrete Wavelet Transform", Berlin, Germany, Springer, 2001.

[16] International Electrotechnical Commission (IEC), 61675- 1, Geneva, Switzerland, 1998. And National Electrical Manufacturers Association (NEMA), Standards Publication No. NU2, Washington, D.C., 2001.

[17] Computed Tomography scanner, King Abdullah university hospital, Ramtha, Jordan, 2009

[18] Shadi AlZubi, Raed Shatnawi and Yaser Jararweh, "Medical Volume Segmentation Using 3D MultiResolution Analysis", In proceeding of: 2012 International Conference on Innovations in Information Technology (IIT), 2012